A Fuzzy Kohonen Local Information C-Means Clustering for Remote Sensing Imagery

Krishna Kant Singh[1], M. J. Nigam[2], Kirat Pal[1] and Akansha Mehrotra[1]

[1]Earthquake Engineering Department, Indian Institute of Technology, Roorkee, India, [2]Electronics and Computer Engineering Department, Indian Institute of Technology, Roorkee, India

ABSTRACT

This paper presents a neuro fuzzy clustering algorithm, Fuzzy Kohonen Local Information C-Means (FKLICM), for classification of remote sensing images. The proposed algorithm is a hybridization of the conventional Kohonen clustering network and Fuzzy Local Information C-Means (FLICM) to produce a much more efficient and accurate clustering algorithm. The proposed algorithm first forms a fused image with three Multispectral bands and pan band of Landsat 7 Enhanced Thematic Mapper Plus (ETM+) using the Brovey transform. The fused image is a three band image with higher resolution and better visual perception. The fused image is reduced to a one-dimensional image using principal component analysis (PCA). The FKLICM algorithm is applied on the PC-1 image to classify the remote sensing image into different land cover types. Integrating the neural network with a fuzzy system combines the advantages and overcomes the limitations of both technologies. The experimental results of the proposed algorithm are compared with two other algorithms, FCM and GIFP-FCM. The classification results and accuracy assessment show that FKLICM yields better results than the other methods.

Keywords:

Brovey transform, Clustering, FCM, FLICM, Kohonen clustering network, PCA.

1. INTRODUCTION

Remote sensing images are widely used in applications such as urban area monitoring and planning, disaster management, climate studies, natural hazard monitoring and land cover monitoring of forest resources. Remote sensing applications employ image classification to identify the different land cover types and assign them a unique grey level to create a thematic image. An important unsupervised classification method is clustering, which groups a set of patterns or vectors into different clusters based on the internal homogeneity and the external separation [1–3]. In recent years, artificial neural networks and fuzzy logic-based methods have been widely used for classification of remote sensing images owing to their inherent advantages over the traditional approaches [4]. Image classification techniques fall under two categories, unsupervised and supervised classification. Supervised classification techniques require analyst-specified training data to perform classification. Unsupervised classification is a technique that analyses a large number of unknown pixels and groups them into homogeneous regions or classes based on natural groupings present in the image values. The widely used unsupervised classifiers are Kohonen clustering network (KCN) [5], fuzzy c-means (FCM) [6, 7] and fuzzy Kohonen clustering network (FKCN) [8, 9]. The KCN, developed by Kohonen, groups the input data into clusters based on competitive learning using the Euclidean distance metric. The cluster unit whose weight vector matches the input vector closely is selected as the winner. The weights of the winning node and its neighbours in the Kohonen layer are updated to more closely resemble the input vector. KCNs have several limitations. FCM and other methods based on FCM perform clustering by optimizing the value of an objective function. The limitation of FCM is that it gets stuck at local optima and an appropriate value of fuzziness index m is required for better performance of FCM. Höppner and Klawonn proposed IFP-FCM, which assigns crisp membership degrees but is less sensitive to noise [10]. Fuzzy local information c-means clustering (FLICM) is an improvement of the FCM algorithm. It introduces a fuzzy factor which improves the clustering results as well as making the algorithm insensitive to noise [11]. Generalized fuzzy c-means clustering algorithm with improved fuzzy partitions (GIFP-FCM) [12] is a generalized form of FCM and IFP-FCM; it provides better clustering and overcomes the limitations of FCM and IFP-FCM. One of the drawbacks of GIFP-FCM is that it is sensitive to noise as it does not take into consideration the spatial information contained in the pixels.

To overcome this problem another clustering algorithm, fuzzy clustering algorithm with nonlocal adaptive spatial constraint (FCA-NLASC) was proposed [13]. FCA-NLASC has a nonlocal adaptive spatial constraint term, which is useful in case of noisy image segmentation. A number of image segmentation techniques are discussed in [14, 15]. In this paper, a fuzzy Kohonen local information c-means clustering (FKLICM) algorithm for classification of remote sensing image is proposed. The algorithm first fuses the multispectral (MS) bands and pan band using the Brovey transform to obtain a higher-resolution image. The fused image contains three bands. Thus, to obtain a single band image, PCA transformation is applied on the fused image and its first component that is the PC-1 image is extracted. The FKLICM clustering algorithm is applied on the PC-1 image to classify it into different classes. FKLICM is a neuro-fuzzy model that combines the Kohonen clustering network with FLICM clustering algorithm. The experimental results show that the proposed hybridized neuro-fuzzy model, FKLICM, is much more efficient and effective for classification of remote sensing images.

2. BACKGROUND

In this section, the Kohonen clustering network, fuzzy c-means and FLICM clustering algorithms are examined to identify their advantages and limitations.

2.1 KCN

The KCN is the simplest neural network, without any activation function and hidden layer. The network has only two layers, the input layer and output layer. The neuron closest to the input vector in terms of Euclidean distance is the winner neuron [5]. The weight of the winner and its predefined neighbours are updated using a learning rule. The operation of KCN is summarized below.

Step 1. Initialization: initialize the cluster centres z_i $(1 \le i \le c)$, learning rate Υ $(0 \le \Upsilon \le 1)$, threshold ε $(\varepsilon > 0)$ and topological neighbourhood parameters.

Step 2. Selection of winner: calculate the squared Euclidean distance for $i = 1, 2, \ldots, c$.

$$d_{ik}^2 = \|x_k - z_i\|^2 \text{ for } k = 1, 2, \ldots, N \quad \text{and} \quad i = 1, 2, \ldots, c \tag{1}$$

where x_k denotes the kth pixel of the input image X and N is the total number of pixels in the image X. The winning output neuron is decided by

$$\min\{d_{ik}^2\} \text{ for } k = 1, 2, \ldots, N \text{ and } i = 1, 2, \ldots c$$

Step 3. Weight update: the weight of the output neuron is updated by

$$z_{1,t} = z_{1,t-1} + \Upsilon_{1k,t}(x_k - z_{1,t-1}) \tag{2}$$

where Υ is learning rate.

Step 4. Update the learning rate Υ

Step 5. If $\|z_{1,t} - z_{1,t-1}\| > \varepsilon$ then go to step 2, otherwise go to step 6.

Step 6. Output the final clustering result.

2.2 FCM

The FCM algorithm is widely used for image clustering [7]. FCM groups the data points into c clusters. Each cluster has a cluster centre, z_i. The cluster centres are computed by means of optimizing the value of an objective function. Each point is assigned a fuzzy membership in the range [0, 1]. However, the sum of the memberships of a point in all clusters is equal to one. The fuzzy membership values are placed in the membership matrix. The FCM algorithm minimizes the objective function, J_m given by Equation (3):

$$J_m = \sum_{k=1}^{N} \sum_{i=1}^{c} u_{ik}^m \|z_i - x_k\|^2 \tag{3}$$

Clustering is done by iteratively optimizing the objective function (J_m). The steps involved in FCM are as follows.

Step 1. Initialize the cluster centres z_i $(1 \le i \le c)$, fuzziness index $m(1 < m \le \infty)$, fuzzy partition matrix U and threshold ε $(\varepsilon > 0)$, number of iterations.

Step 2. Calculate the fuzzy membership matrix $U = [u_{ik}]$ by Equation (4):

$$u_{ik} = \left(\sum_{l=1}^{c} \left(\frac{\|z_i - x_k\|}{\|z_l - x_k\|} \right)^{2/(m-1)} \right)^{-1} \tag{4}$$

for $1 \le i \le c$ and $1 \le k \le N$, where c is the number of clusters, x_k denotes the k_{th} pixel of the input image X and N is the total number of pixels in the image X.

Step 3. The cluster centres are updated by Equation (5):

$$z_i = \frac{\sum_{k=1}^{N} u_{ik}^m x_k}{\sum_{k=1}^{N} u_{ik}^m} \tag{5}$$

Step 4. If $\|U^{t+1} - U^t\| > \varepsilon$ then go to step 2, otherwise go to step 5.

Step 5. Output the final clustered image by assigning the pixel x_k to the class c with highest membership value.

The limitation of FCM is that its performance depends upon the choice of fuzziness index m. An inappropriate value of m leads to unsatisfactory results. The inability of FCM to consider local spatial information makes it highly sensitive to noise. Thus, FCM performs poorly in the case of noisy images.

2.3 FLICM

To further improve the performance of FCM, a new clustering technique named FLICM was introduced by Kirindis and Chatzis [11]. It uses the local spatial and grey-level information in its objective function. The objective function of FLICM is given by Equation (6):

$$J_m = \sum_{k=1}^{N}\sum_{i=1}^{c}\left[u_{ik}^m\|z_i - x_k\|^2 + \alpha_{ik}\right] \tag{6}$$

The fuzzy factor α_{ik} is mathematically expressed as follows:

$$\alpha_{ik} = \sum_{j\in N_r}\frac{1}{d(k,j)+1}\,(1-u_{ij})^m\|z_i - x_j\|^2 \tag{7}$$

where the kth pixel of the input image X is the centre of the local window N_r, x_j represents the neighbourhood pixels and $d(k,j)$ is the spatial Euclidean distance between pixels k and j. The fuzzy membership matrix $U = [u_{ik}]$ is computed using Equation (8):

$$u_{ik} = \left(\sum_{l=1}^{c}\left(\frac{\|z_i - x_k\|^2 + \alpha_{ik}}{\|z_l - x_k\|^2 + \alpha_{lk}}\right)^{1/(m-1)}\right)^{-1} \tag{8}$$

for $1 \le i \le c$ and $1 \le k \le N$.

where x_k denotes the kth pixel of the input image X and N is the total number of pixels in the image X.

The cluster centres are updated by Equation (9):

$$z_i = \frac{\sum_{k=1}^{N} u_{ik}^m x_k}{\sum_{k=1}^{N} u_{ik}^m} \tag{9}$$

On convergence of the algorithm, the pixels of the image are assigned to the class with highest membership value to obtain the classified image.

3. PROPOSED ALGORITHM

The proposed algorithm consists of two main steps:

1. image fusion and dimensionality reduction;
2. FKLICM.

These are discussed in the following sections. The flowchart of the proposed algorithm is shown in Figure 1.

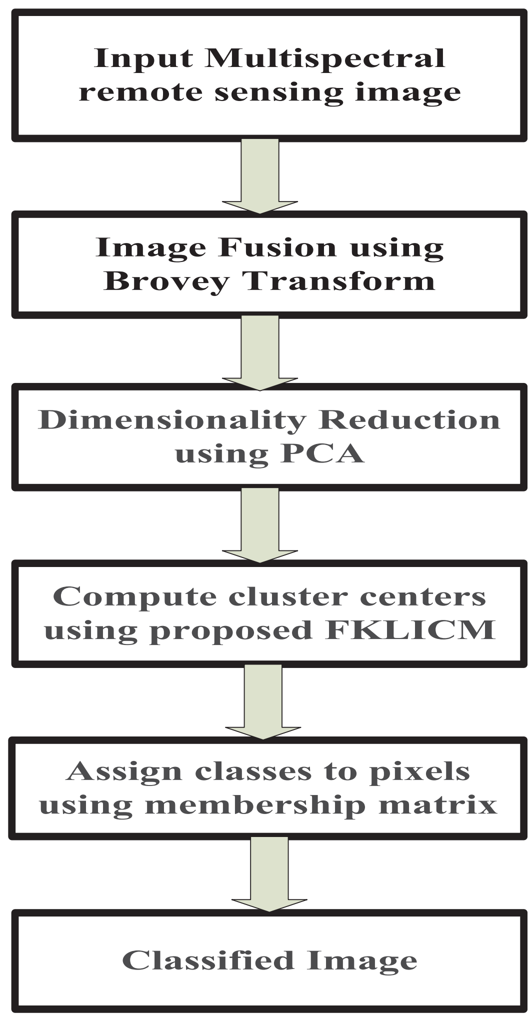

Figure 1: Flowchart of the proposed algorithm.

3.1 Image Fusion and Dimensionality Reduction

Satellite images consist of multiple number of bands. These bands contain complementary information. Image fusion is done to combine the information in different bands into one image. The new image obtained is more appropriate for further processing as it has higher resolution and better visual quality. In this paper, Brovey transformation [16] is used to fuse the RGB bands of the MS image with the pan band. Brovey transformation is a numerical technique that uses a ratio algorithm to fuse images. The mathematical definition of Brovey transformation is given in Equation (10):

$$I_{fuse,n}(i,j) = \frac{I_n(i,j)I_{pan}(i,j)}{\sum_{n=1}^{3} I_n(i,j)} \tag{10}$$

where $I_{fuse,n}$ is the nth band of the fused image, I_n is the nth original MS band image and I_{pan} is the original band image. In this paper, a Landsat 7 ETM+ image is used, which consists of eight bands as shown in Table 1 [17]. Thus, the value of n ranges from 1 to 3 in Equation (10).

The fused image is a three-dimensional image consisting of three bands and can be expressed as 3D column vector, I_{fuse}:

$$I_{\text{fuse}}(x,y) = \begin{bmatrix} I_{\text{fuse},1} \\ I_{\text{fuse},2} \\ I_{\text{fuse},3} \end{bmatrix} \tag{11}$$

Further, the first component (PC-1) of principal component analysis (PCA) [18–20] is used to reduce the dimensionality of the image to one dimension. If the images are of size $H \times W$ there will be total of HW such vectors comprising all of the pixels in the images. For simplicity, I^k_{fuse} is used to represent the vector $I_{\text{fuse}}(x,y)$, while k represents an index with $1 \le k \le N$

Table 1: Landsat 7 ETM+ bands

Band number	Spectral range (μm)	Ground resolution (m)
1	0.45–0.515	30
2	0.52– 0.605	30
3	0.63–0.69	30
4	0.75–0.90	30
5	1.55–1.75	30
6	10.40–12.5	60
7	2.09–2.35	30
Pan	0.52–0.90	15

where $N = H \times W$. To create the feature vector using PCA, we proceed as follows. The average vector, χ, of a vector population can be approximated by

$$\chi = \frac{1}{N}\sum_{k=1}^{N} I^k_{\text{fuse}} \tag{12}$$

The difference between the each vector and average vector is $\Delta_k = I^k_{\text{fuse}} - \chi$. The covariance matrix C_I has eigenvectors e_i and corresponding eigenvalues λ_i. The covariance matrix C_I can be approximated by

$$C_I = \frac{1}{N-1}\sum_{k=1}^{N} \Delta_k \Delta_k^{\text{T}} \tag{13}$$

where we use $N-1$ instead of N to obtain an unbiased estimate of C_I. It is assumed that the generated eigenvectors of C_I are sorted in decreasing order based on the eigenvalues, that is, $\lambda_i \ge \lambda_{i+1}$.

The feature vector space is obtained by projecting $I_{\text{fuse}}(x,y)$ onto eigenvector space for each pixel at spatial location (i, j) using PCA, that is,

$$X(i,j) = \begin{bmatrix} X_1(i,j) \\ X_2(i,j) \\ X_3(i,j) \end{bmatrix} = A\Big(I_d(x,y) - \chi\Big) \tag{14}$$

The eigenvectors of C_I are arranged as rows of the matrix A. The first row of the matrix is the eigen vector with the largest eigenvalue and so on. X_1 is the PC-1 image obtained from Equation (14).

3.2 FKLICM

A FKLICM is proposed in this paper. FKLICM uses a neuro-fuzzy hybrid approach. It is a hybridization of KCN with FLICM. KCN is the simplest neural network, without any activation function and hidden layer. Thus, hybridizing KCN with FLICM is less complex than other neuro-fuzzy systems. The use of a neuro-fuzzy method overcomes the limitations of conventional methods and has the advantages of both neural networks and fuzzy systems. To integrate FLICM with KCN, the following algorithm is used.

Step 1. Initialize the cluster centres z_i $(1 \le i \le c)$, the threshold ε $(\varepsilon > 0)$ and topological neighbourhood parameters. Set $t = 1$, maximum iteration limit $t_{\max}$ and $m > 1$.

Step 2. Calculate m_t, fuzzy membership matrix $U = [u_{ik}]$ and learning rate $\Upsilon_{ik,t}$, , using Equations (15)–(17) respectively.

$$m_t = m + \frac{t(m-1)}{t_{\max}} \tag{15}$$

$$u_{ik} = \left(\sum_{l=1}^{c} \left(\frac{\|z_i - x_k\|^2 + \alpha_{ik}}{\|z_l - x_k\|^2 + \alpha_{lk}} \right)^{1/(m_t-1)} \right)^{-1} \tag{16}$$

for $1 \le i \le c$ and $1 \le k \le N$. x_k denotes the kth pixel of the PC-1 image X_1 and α_{ik} is calculated using Equation (7).

$$\Upsilon_{ik,t} = (u_{ik})^{m_t} \tag{17}$$

Step 3. The weight of the output neuron is updated by

$$z_{i,t} = z_{i,t-1} + \frac{\sum_{k=1}^{N} \Upsilon_{ik,t}(x_k - z_{i,t-1})}{\sum_{s=1}^{N} \Upsilon_{is,t}} \tag{18}$$

Step 4. Update the learning rate $\Upsilon_{ik,t}$.

Step 5. Set $t = t + 1$.

Step 6. If $\|z_{1,t} - z_{1,t-1}\| > \varepsilon$ and $t < t_{\max}$ then go to step 2, otherwise go to step 7.

Step 7. Output the final clustered image by assigning the pixel x_k to the class c with highest membership value.

The use of spatial contextual information makes the algorithm less sensitive to noise. Also, the inter cluster distance is large enough, avoiding overlapping of clusters. The network architecture consists of two layers: input layer and output layer. The input layer consists of N neurons; the kth neuron represents the kth pixel of the image to be clustered. The output of the network is c neurons corresponding to the c cluster centres. The architecture of the network is shown in Figure 2.

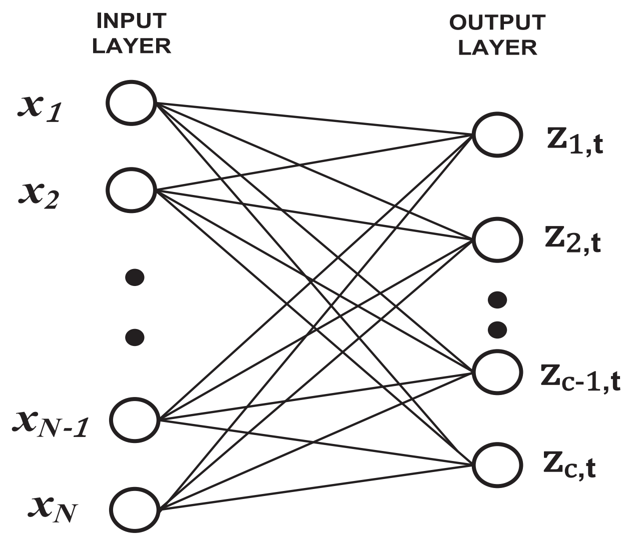

Figure 2: Network architecture of FKLICM.

4. EXPERIMENTAL RESULTS

In this section, the performance of the FKLICM is evaluated. The algorithm was implemented in Matlab R2012b. The experiment was conducted on Landsat 7 ETM+ image with eight bands over Ishinomaki City, Japan, acquired on 18 February 2003 (image courtesy US Geological Survey) [21]. The study image is shown in Figure 3(a). The geographical coordinates of the area are 38° 25′ 0″ North, 141° 18′ 0″ East. To test the performance of the proposed FKLICM, it is compared with FCM and GIFP-FCM. The classification results are shown in Figure 3. The various parameters used in the experiment are $c = 3$, $m = 2$, $\varepsilon = 1 \times 10^{-6}$. The qualitative analysis of the results shows that FKLICM gives better results than the other two methods. Further, the accuracy assessment of FKLICM, FCM and GIFP-FCM was performed using ERDAS™ software. An error matrix was used for a series of descriptive and analytical statistical analyses. Overall accuracy and kappa coefficient were used for the assessment of the proposed algorithm. A total of 256 reference points were chosen using stratified random sampling.

The error matrices of all the three methods are given in Table 2 where classes 1–3 represent vegetation, land and urban area, and water, respectively. The error matrix shows that the number of misclassifications in FKLICM is minimal while GIFP-FCM shows improvement over FCM. The overall accuracy is 96.88 and the kappa coefficient is 0.9485 for FKLICM, which is higher than the other two methods. Thus, the quantative and qualitative analysis shows that the proposed FKLICM provides better accuracy and classification results.

The kappa coefficient value lies between 0 and 1. The higher the value of kappa, the higher the classification accuracy is. Accuracy and kappa coefficient values of the three methods are listed in Table 3. It can be seen that FKLICM has highest overall accuracy and highest value of kappa coefficient, conforming that the proposed method outperforms the other two.

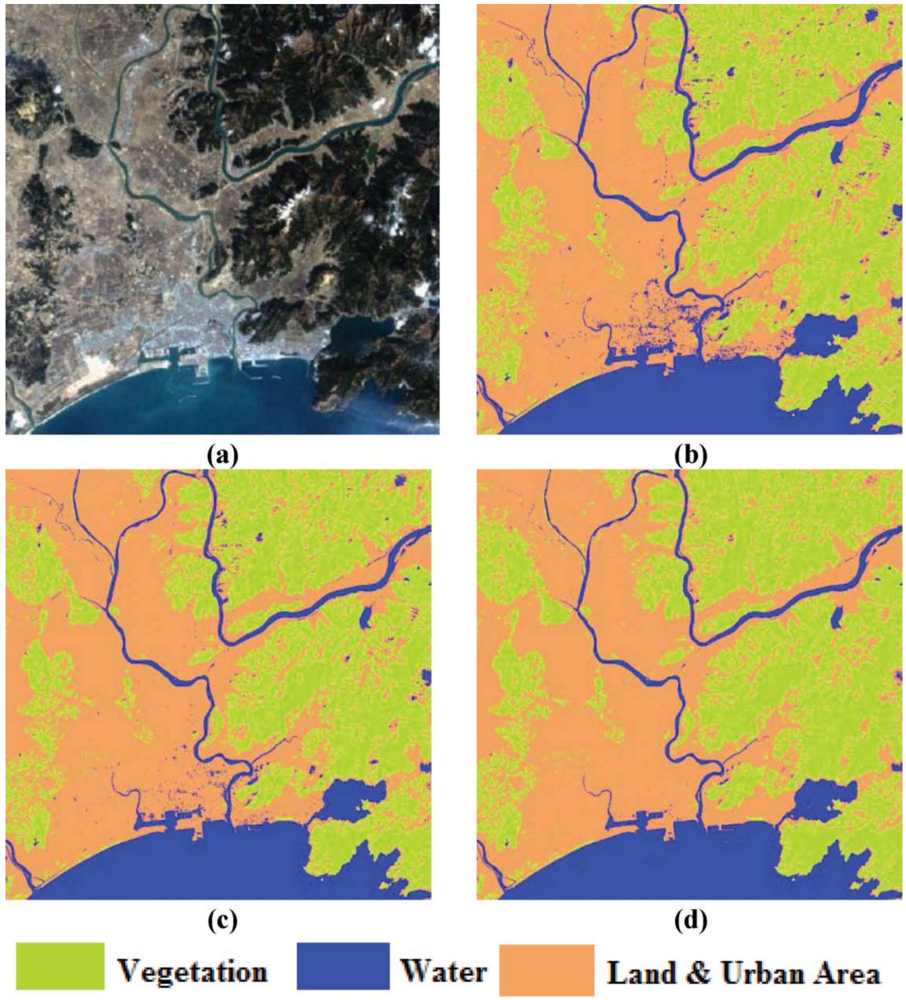

Figure 3: (a) Original Landsat 7 ETM+ image; (b) classified image with FCM; (c) classified image with GIFP-FCM, $\alpha = 0.7$; (d) classified image with FKLICM.

Table 2: Error matrix

Method		Class 1	Class 2	Class 3
FCM	Class 1	96	7	1
	Class 2	4	109	4
	Class 3	2	3	30
GIFP-FCM	Class 1	99	4	1
	Class 2	2	112	3
	Class 3	1	3	31
FKLICM	Class 1	102	1	1
	Class 2	2	114	1
	Class 3	1	2	32

Table 3: Accuracy and kappa

Method	Overall accuracy	Kappa
FCM	91.80	0.8649
GIFP-FCM	94.53	0.9099
FKLICM	96.88	0.9485

5. CONCLUSION

In this paper, a novel clustering algorithm, FKLICM, for classifying remote sensing images is proposed. FKLICM is a neuro-fuzzy hybridization of KCN and FLICM. The input image is first fused using Brovey transformation to convert it into a three-band image having higher resolution, and is visually more enhanced. This three-band image is converted into a single-band image using PCA. The PC-1 image is then classified into different classes using the FKLICM algorithm. The use of a neuro-fuzzy model embeds the advantages of neural networks as well as those of fuzzy systems. The local information makes it less sensitive to noise and also improves clustering performance. Experimental results and accuracy assessment show that FKLICM gives better overall accuracy and kappa as compared with other state-of-the-art methods.

REFERENCES

1. P. Hansen, and B. Jaumard, "Cluster analysis and mathematical programming," *Math. Program.*, Vol. 79, 1997, pp. 191–215.
2. A. Jain, and R. C. Dubes, *Algorithms for Clustering Data*. Englewood Cliffs, NJ: Prentice-Hall, 1988.
3. R. Xu, and D. Wunsch, "Survey of clustering algorithms," *IEEE Trans. Neural Networks*, Vol. 16, no. 3, pp. 645–78, 2005.
4. J. F. Mas, and J. J. Flores, "The application of artificial neural networks to the analysis of remotely sensed data," *Int. J. Remote Sensing*, Vol. 29, no. 3, pp. 617–63, 2008.
5. T. Kohonen, *Self-Organization and Associative Memory*, 3rd edn. Springer, Berlin, 1989.
6. M. Filippone, F. Camastra, F. Masulli, and S. Rovetta, "A survey of kernel and spectral methods for clustering," *Pattern Recognit.*, Vol. 41, no. 1, pp. 176–90, 2008.
7. J. C. Bezdek, *Pattern Recognition with Fuzzy Objective Function Algorithms*. New York: Plenum Press, 1981.
8. E. C. Tsao, J. C. Bezdek, and N. R. Pal, "Fuzzy Kohonen clustering network," *Pattern Recognit.*, Vol. 27, no. 5, pp. 757–64, 1994.
9. C. Zhang, and F. Qiu, "Hyperspectral image classification using an unsupervised neuro-fuzzy system," *J. Appl. Remote Sensing*, Vol. 6, no. 1, p. 063515–1, 2012.
10. F. Höppner, and F. Klawonn, "Improved fuzzy partitions for fuzzy regression models," *Int. J. Approx. Reason.*, Vol. 32, no. 2, pp. 85–102, 2003.
11. S. Kirindis, and V. Chatzis, "A robust fuzzy local information c means clustering algorithm," *IEEE Trans. Image Process.*, Vol. 19, no. 5, pp. 1328–37, 2010.
12. L. Zhu, F. L. Chung, and S. Wang, "Generalized fuzzy c-means clustering algorithm with improved fuzzy partitions," *IEEE Trans. System, Man Cybernet. Pt B: Cybernet.*, Vol. 39, no. 3, pp. 578–91, 2009.
13. F. Zhao, L. Jiao, H. Liu, and X. Gao, "A novel fuzzy clustering algorithm with non local adaptive spatial constraint for image segmentation," *Signal Process.*, Vol. 91, no. 4, pp. 988–99, 2011.
14. K. K. Singh, and A. Singh, "A study of image segmentation algorithms for different types of images," *Int. J. Comput. Sci. Issues*, Vol. 7, no. 5, September 2010.
15. D. Jayadevappa, S. S. Kumar, and D. S. Murty, "Medical image segmentation algorithms using deformable models: A review," *IETE Tech. Rev.*, Vol. 28, no. 3, pp. 248–55, 2011.
16. S. Dahiya, P. K. Garg, and M. K. Jat, "A comparative study of various pixel-based image fusion techniques as applied to an urban environment," *Int. J. Image Data Fusion*, pp. 1–17, 2013.
17. National Aeronautics and Space Association. Available: http://landsat.gsfc.nasa.gov/about/etm+.html
18. R. C. Gonzalez, and R. E. Woods, *Digital Image Processing*. Englewood Cliffs, NJ: Prentice-Hall, 2008.
19. T. Celik, "Unsupervised change detection in satellite images using principal com-ponent analysis and k-means clustering," *IEEE Geosci. Remote Sensing Lett.*, Vol. 6, no. 4, pp. 772–6, 2009.
20. K. K.Singh, A. Mehrotra, M. J. Nigam, and K. Pal, "Unsupervised change detection from remote sensing images using hybrid genetic FCM" in *Proceedings of 2nd Students' Conference on Engineering and Systems (SCES2013)*, April 2013, pp. 423–7.
21. USGS Global Visualization Viewer. Available: http://glovis.usgs.gov

Authors

Krishna Kant Singh is currently pursuing a PhD from Indian Institute of Technology, Roorkee, India. He holds BTech (EI) and MTech (VLSI) degrees. His areas of specialization include digital image processing, VLSI technology and neural networks. He has authored more than 12 research papers in the above areas in national and international journals and conferences.

E-mail: krishnaiitr2011@gmail.com

Madhav J. Nigam is a professor in the Electronics and Computer Engineering Department, Indian Institute of Technology, Roorkee, India. His areas of research include digital image processing, control systems and neural networks. He has authored a number of research papers in the above-mentioned areas.

E-mail: mkndnfec@gmail.com

Kirat Pal is a professor in the Earthquake Engineering Department of the Indian Institute of Technology Roorkee. He has authored more than 61 research papers in national and international journals and conferences.

E-mail: kiratfeq@iitr.ernet.in

Akansha Mehrotra is currently pursuing a PhD from Indian Institute of Technology, Roorkee, India. She has to her credit a number of research papers in international conferences and journals. Her areas of interest include digital image processing, remote sensing and neural networks.

E-mail: akanshasing@gmail.com

DOI: 10.1080/02564602.2014.891375;